

Discovery of Thioether-Cyclized Macrocyclic Covalent Inhibitors by mRNA Display

Tong Lan, Cheng Peng, Xiyuan Yao, Rachel Shu Ting Chan, Tongyao Wei, Anuchit Rupanya, Aleksandar Radakovic, Sijie Wang, Shiyu Chen, Scott Lovell, Scott A. Snyder, Matthew Bogyo, and Bryan C. Dickinson*



Cite This: *J. Am. Chem. Soc.* 2024, 146, 24053–24060



Read Online

ACCESS |



Metrics & More

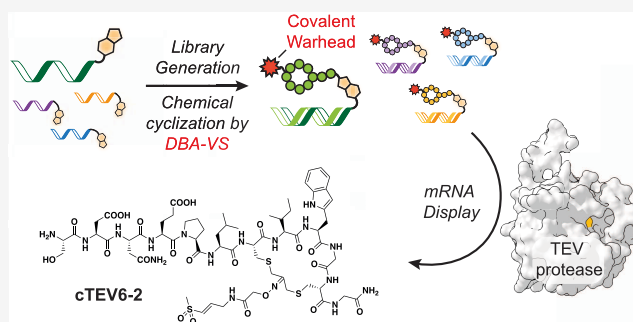


Article Recommendations



Supporting Information

ABSTRACT: Macrocyclic peptides are promising scaffolds for the covalent ligand discovery. However, platforms enabling the direct identification of covalent macrocyclic ligands in a high-throughput manner are limited. In this study, we present an mRNA display platform allowing selection of covalent macrocyclic inhibitors using 1,3-dibromoacetone-vinyl sulfone (DBA-VS). Testcase selections on TEV protease resulted in potent covalent inhibitors with diverse cyclic structures, among which cTEV6-2, a macrocyclic peptide with a unique C-terminal cyclization, emerged as the most potent covalent inhibitor of TEV protease described to-date. This study outlines the workflow for integrating chemical functionalization—installation of a covalent warhead—with mRNA display and showcases its application in targeted covalent ligand discovery.



INTRODUCTION

Inhibitors that covalently target nucleophiles in biomacromolecules, most notably cysteine residues in proteins, have revolutionized chemical probe design and modern drug discovery.^{1–3} The ligandability and functionality of cysteine residues across the proteome have been extensively profiled using unbiased approaches, indicating which cysteines are likely to be viable and useful targets for covalent inhibitors.^{4–9} Fragment-based covalent probes can be identified and used as a starting point for inhibitor design and to confirm functional outcomes *in cellulo*.^{5,9–11} However, extensive screening efforts are still necessary to identify the fragment-based probes targeting a specific cysteine-of-interest, and advanced development of fragments into potent inhibitors remains a time- and labor-consuming process.

Macrocyclic peptides are useful scaffolds for ligand discovery, as their peptidic nature and constrained conformation allow them to target both deep pockets and shallow protein surfaces with high specificity and affinity.^{12–14} More importantly, the ability to easily generate large numbers of random peptides, modify those peptides for diverse structures, and perform selections with various high-throughput enrichment-based technologies enables rapid discovery of macrocyclic ligands that bind to targets of interest.^{15–22} While previous successes and current clinical trials of macrocyclic peptides primarily focus on noncovalent macrocyclic ligands,^{23–25} covalently targeting cysteine residues with macrocyclic peptide scaffolds holds promise for identification of

highly specific ligands capable of targeting a functional cysteine residue of interest. Pioneering work has demonstrated the feasibility of direct identification of potent covalent macrocyclic ligands with display technologies, for example, using cysteine-targeting warheads in cyclic peptide libraries with phage display.^{26–28} More recently, the incorporation of covalent warheads has been successfully applied to mRNA display using non-natural amino acids for covalent ligand selection.^{29–31} Beyond the identification of useful cysteine-targeting covalent scaffolds for chemical probe discovery or early stage drug development, these efforts, although still sparse, have nonetheless revealed the power of display technologies with macrocyclic peptides in covalent ligand discovery.

Here we present a tractable mRNA display workflow that allows cyclization and cysteine-targeting covalent warhead installation via a chemical linker, 1,3-dibromoacetone-vinyl sulfone. Using this workflow, we demonstrate the direct selection of functional covalent ligands targeting TEV protease, a testbed cysteine hydrolase. We discovered a highly potent, covalent TEV protease inhibitor, cTEV6-2, which contains an

Received: June 10, 2024

Revised: August 6, 2024

Accepted: August 7, 2024

Published: August 13, 2024



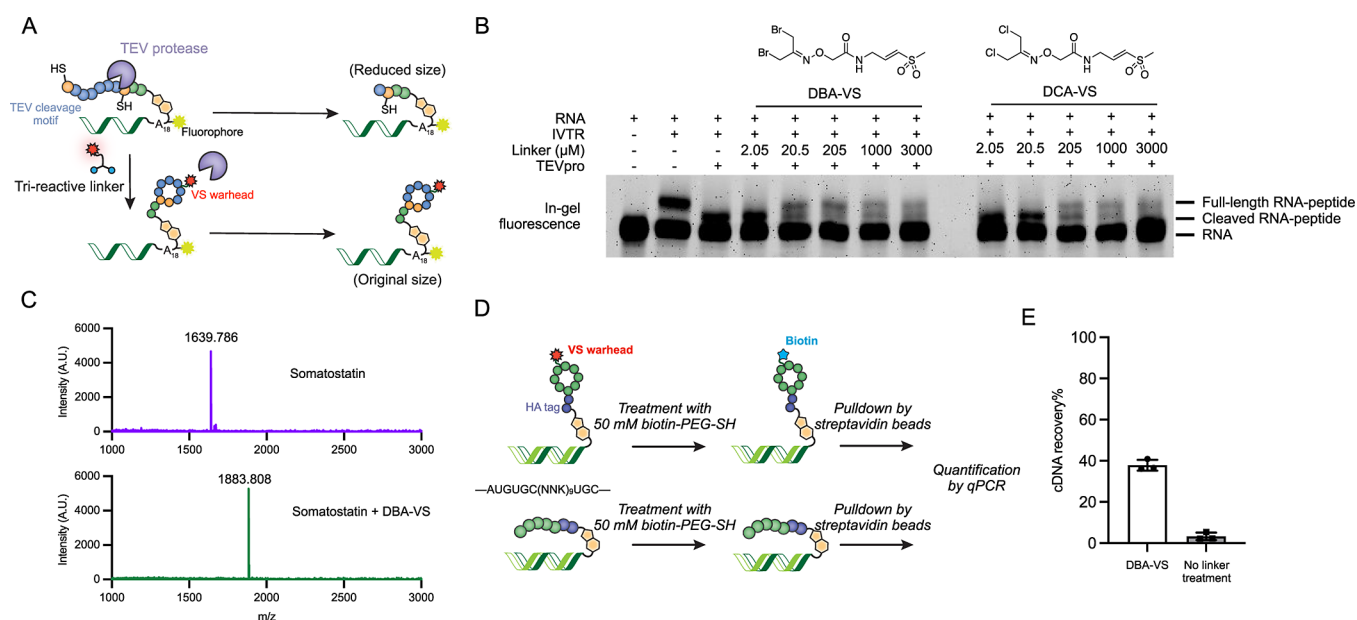


Figure 1. mRNA display platform using the DBA-VS linker for covalent ligand selection. (A) Schematic of TEV cleavage assay for assessing the cyclization efficiency on peptides containing Cys-Glu-Asn-Leu-Tyr-Phe-Gln-Ser-Cys (CENLYFQSC) displayed on mRNA. (B) Fluorescence gel from TEV cleavage assay with mRNA-peptide in (A) after a 30 min treatment of 1,3-dibromoacetone-vinyl sulfone (DBA-VS, 0–3000 μM) or 1,3-dibromoacetone-vinyl sulfone (DCA-VS, 0–3000 μM). $n = 2$. (C) MALDI traces of 10 μM somatostatin (Ala-Gly-Cys-Lys-Asn-Phe-Phe-Trp-Lys-Thr-Phe-Thr-Ser-Cys) with or without a 30 min treatment of 205 μM DBA-VS in TE, pH 8.0, with 0.2 mM TCEP. (D) Schematic and (E) qPCR result of biotin conjugation assay on cDNA:mRNA-peptide encoding Cys(NNK)₉Cys library for assessing the efficiency of thiol-targeting warhead installation after a 30 min treatment with 205 μM DBA-VS, $n = 3$.

unusual C-terminal cyclization, with the strongest potency reported to-date for this target.

RESULTS AND DISCUSSION

Establishing an mRNA Display Platform for Covalent Macrocyclic Ligand Discovery with 1,3-Dibromoacetone-vinyl Sulfone. To leverage the mRNA display platform for discovering covalent inhibitors, we chose to use a small molecule linker that both cyclizes the peptide via a bis-electrophilic moiety and installs a covalent cysteine-targeting warhead in one step. We coupled this with a dicysteine peptide library displayed on mRNA for functionalization and selection, reasoning that this combination will allow full utilization of the high selectivity and target affinity of macrocyclic peptides,³² and also enable them to target both surface and internal cysteine residues on a given target protein.^{26,33} Chemical cyclization on a dicysteine library has previously been established for both noncovalent and covalent ligands with phage display,^{26–28,34–37} as well as noncovalent ligands with mRNA display.^{20,38–42} However, similarly designed covalent warhead installation has not been adapted to mRNA display, where substantially larger library sizes are available to, in principle, enhance the selection scope and hit rate.^{23,43}

The use of a trireactive linker—two reactive sites for cysteine modification and one with a relatively inert covalent warhead—requires tandem purification during selection. This necessitates a high efficiency approach with low bias toward specific sequences and minimal perturbation to the structure of the desired nucleic acid-peptide conjugate. Inspired by previous work,^{38,44,45} we covalently ligated a DNA tag comprised of a poly-A tail, fluorophore, PEG spacer, and puromycin,⁴⁶ with the 3' end of mRNA (Table S1). This DNA tag allows for reversible purification by oligo-dT beads via the universal poly-A tail,⁴⁷ and also mediates the fusion of the

translated peptide with the encoding mRNA in a high-salt environment.⁴⁸ Moreover, the fluorophore facilitates tracking of the translated product and modification on ligated mRNA via a fluorescence gel. To prevent unwanted cross-linking of the covalent warhead with proteins present in *in vitro* translation and reverse transcription reactions, cyclization was performed after reverse transcription. The entirety of library preparation, from ligated mRNA to a fully functionalized library, including three purifications via oligo-dT beads and recovery by gentle heating, can be carried out in standard Eppendorf or PCR tubes and completed in less than 3 h (Figure S1A).

After confirming the tractability of the system via fluorescence gel and establishing the library preparation workflow (Figure S1 and Supplementary text), we used a 1,3-dichloroacetone-vinyl sulfone (DCA-VS) linker to both cyclize and introduce a cysteine-targeting vinyl sulfone warhead. The DCA-VS linker has been previously used to generate phage-encoded peptide libraries.²⁶ We evaluated the cyclization efficiency of the covalent warhead-bearing linker on mRNA-peptide conjugates via the TEV cleavage assay (Figure 1A). In brief, mRNA encoding a TEV cleavage motif (ENLYFQS) flanked by two cysteine residues was ligated with the DNA tag and translated *in vitro* to obtain the corresponding mRNA-peptide conjugate. After incubating mRNA-peptide with various concentrations of DCA-VS linker, excess TEV protease was added to the reaction mixture. Cyclization was quantified via fluorescence gel; linear, i.e., nonreacted, peptides were cleaved in the presence of TEV and reduced in size, while cyclized peptides were not. At DCA-VS concentrations less than 20.5 μM, we observed 10% cyclized product, with peak levels of cyclization (30%) occurring at 205 μM DCA-VS. Higher linker concentrations led to unwanted polymerization (Figures 1B and S2).

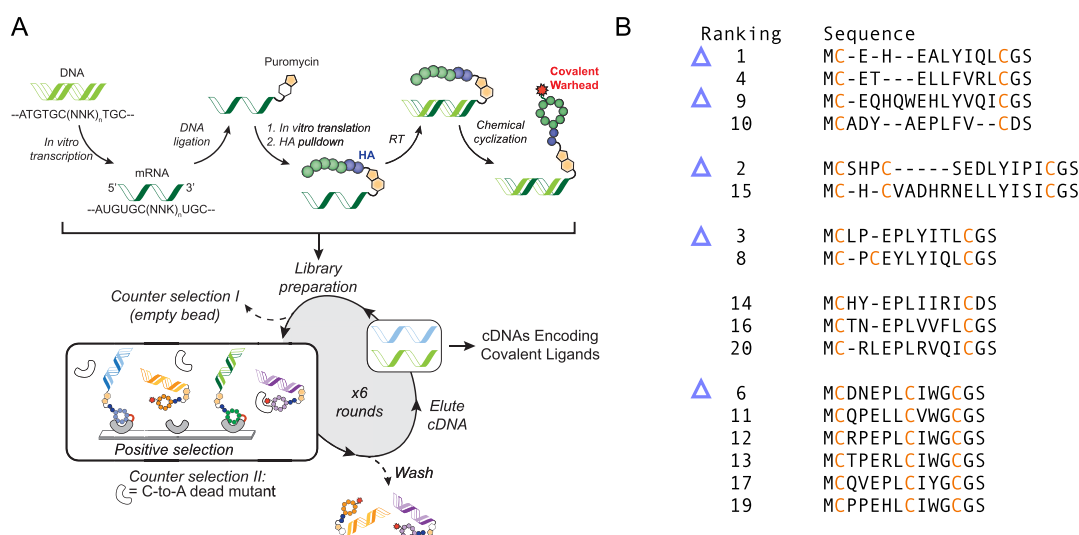


Figure 2. Selection with Cys(NNK)_nCys ($n = 9, 12, 15$) library on TEV protease. (A) Schematic of improved mRNA display workflow using Cys(NNK)_nCys ($n = 9, 12, 15$) library on TEV protease. (B) Multiple sequence alignment of TEV protease-preferred sequences from among the top 20 hits in Figure S7B. Peptides with representative core sequences in each group were selected for further validation and are indicated with purple triangles.

We reasoned that a more reactive cyclizing moiety would improve cyclization at lower linker concentrations, with minimal side product generation.⁴⁹ We synthesized 1,3-dibromoacetone-vinyl sulfone (DBA-VS), which contains a dibromo-imine moiety that is, in principle, more reactive than the dichloro-imine moiety of DCA-VS. Facile synthesis of DBA-VS was achieved over 3 steps (see Methods). With DBA-VS in hand, we examined the reactivity of DBA-VS with cysteines on a model peptide, somatostatin (Ala-Gly-Cys-Lys-Asn-Phe-Phe-Trp-Lys-Thr-Phe-Thr-Ser-Cys). MALDI confirmed the formation of the expected cyclized product on somatostatin. Importantly, we did not observe any byproduct formation on nucleophilic residues other than cysteine on somatostatin, even in the presence of 20-fold excess DBA-VS linker (Figure 1C), confirming cysteine-specific cyclization of the dibromo-imine moiety without cross-reactivity of the vinyl sulfone warhead with cysteines on the peptide. Using the TEV cleavage assay, we then evaluated DBA-VS and DCA-VS in parallel on the CENLYFQSC peptide displayed on mRNA. Compared with DCA-VS, DBA-VS showed a wider effective concentration window and higher cyclization efficiency (53% cyclization at 20.5 μ M and 40% at 205 μ M DBA-VS, respectively) with no observable polymerization (Figures 1B and S2). DBA-VS can therefore serve as a more suitable linker for covalent inhibitor selection via the mRNA display. To further evaluate the performance of DBA-VS on a random library in the context of mRNA display, we treated both 25 nM of a fully functionalized Cys_XCys ($X = \text{NNK}$) library (generated with 205 μ M DBA-VS for 30 min) and an uncyclized library with 50 mM biotin-PEG-SH for 2.5 h, enriched biotinylated species with streptavidin beads, and quantified recovered cDNA by quantitative PCR (qPCR) (Figure 1D). We observed 40% cDNA recovery from the DBA-VS-treated library versus 3% cDNA recovery from the uncyclized library, confirming installation of thiol-targeting covalent warhead via DBA-VS on the random library displayed on mRNA (Figure 1E).

Pilot Selection on TEV Protease with Cys(NNU)₉Cys Library. We next used the well-studied TEV protease as a

benchmark to test our covalent mRNA display platform. We first performed mRNA display on TEV protease with the Cys(NNU)₉Cys library (NNU library). NNU codons exclude stop codons and include 15 out of 20 natural amino acid residues, and NNU libraries have been proven useful in previous mRNA display selections.^{29,50} We performed four rounds of selection using the NNU library, starting with $\sim 4 \times 10^{12}$ unique sequences and enrichment with immobilized TEV protease (Figure S3A). We incubated the library with TEV protease overnight in the first two rounds to efficiently capture as many binders as possible, and added a counter selection (empty streptavidin beads) starting from the second round to remove nonspecific binders. As with previously described covalent peptide selections,^{26,29} we also performed a denaturing wash with 5 M guanidine before cDNA elution in every round to remove as many noncovalent binders as possible.

We observed first a decrease and then an increase in cDNA recovery over four rounds (Figure S3B). A comparative pulldown revealed TEV protease-dependent enrichment at the fourth round (Figure S3C,D). However, next-generation sequencing (NGS) data revealed that although the “two-Cys” structure was, for the most part, retained, there were no apparent consensus sequences in the NNU randomized region (Figure S4). The majority of enriched species instead shared a previously defined TEV protease binding motif, EPLY, in the designed constant region encoding an HA tag (YPYDVPDY),²⁶ not the NNU randomized region. This was likely due to a mutation or deletion of the HA tag-encoding sequence, which we had included to detect the translated product during our previous workflow optimization.

Selection on TEV Protease with Cys(NNK)_{9,12,15}Cys Library. The unexpected enrichment of the EPLY motif outside the randomized region suggested that while our workflow was able to enrich binders, a more restricted quality control over translation is required during selection to obtain desired covalent ligands. The restricted preference of TEV protease to the EPLY motif, which is excluded in the NNU library, necessitates a library with better codon coverage to

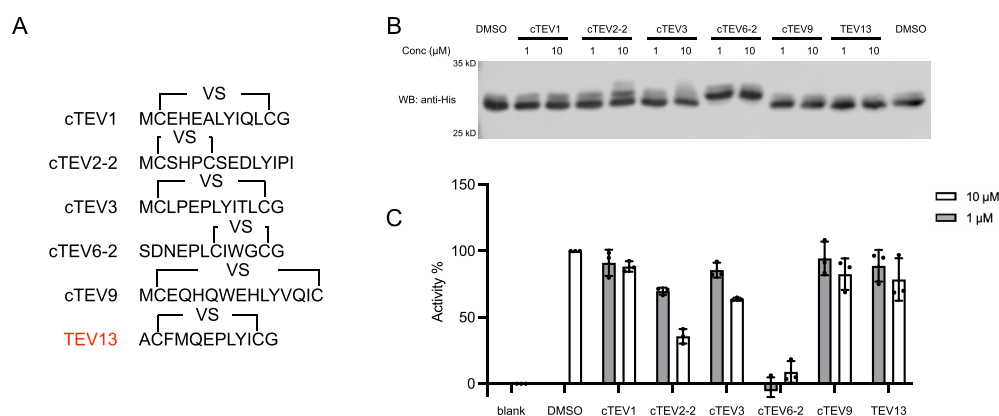


Figure 3. Discovery of covalent inhibitors for TEV protease via selection. (A) Sequences and structures of five representative hits and TEV13²⁶ synthesized for validation. (B) Covalent engagement of molecules in (A) with 150 nM TEV protease after a 1 h incubation at 30 °C examined by the size change of TEV protease on SDS-PAGE followed by Western Blot. $n = 2$. (C) Evaluation of molecules in (B) against 150 nM TEV protease enzymatic activity using 5 μM Cy5-ENLYFQGK(QSY21)-NH₂ after a 1 h preincubation at 30 °C. Data represent mean ± S.D., with individual data points shown, $n = 3$.

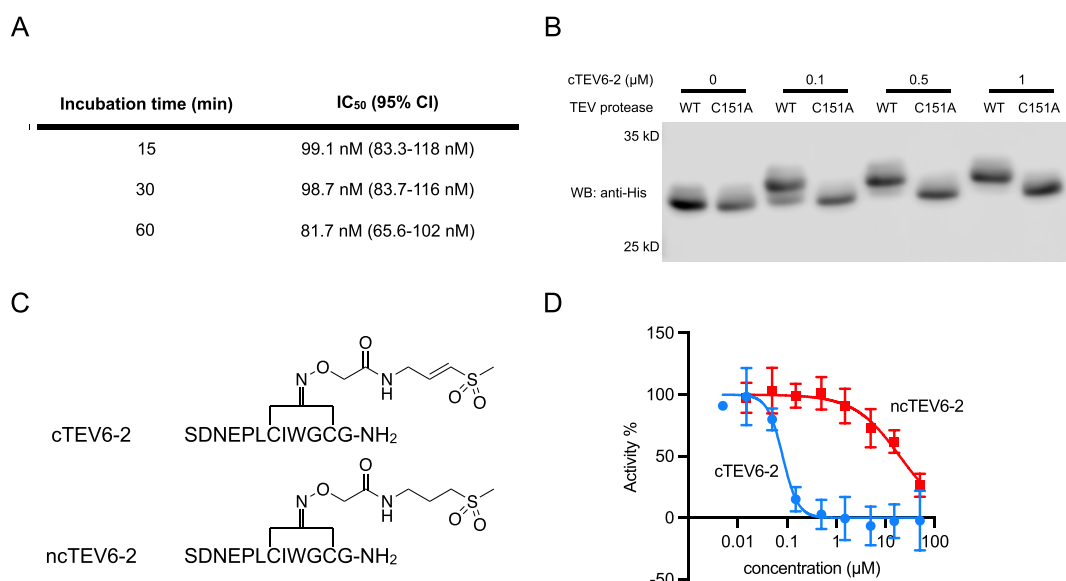


Figure 4. CTEV6-2 as potent covalent inhibitor to TEV protease. (A) IC₅₀ under 15-, 30-, and 60 min preincubation of cTEV6-2 with 150 nM TEV protease using 5 μM Cy5-ENLYFQGK(QSY21)-NH₂ at 30 °C, $n = 3$. (B) Covalent engagement of cTEV6-2 with 150 nM wild-type TEV protease or TEV protease C151A mutant after a 1 h incubation at 30 °C examined by the size change of TEV protease on SDS-PAGE, followed by Western Blot, $n = 2$. (C) Structures of cTEV6-2 and ncTEV6-2. (D) Dose–response curves of cTEV6-2 and ncTEV6-2 on 150 nM TEV protease enzymatic activity using 5 μM Cy5-ENLYFQGK(QSY21)-NH₂ after a 1 h preincubation at 30 °C. Data are the mean ± S.D., $n = 3$.

successfully select the desired structures. Furthermore, this illustrates that randomized codon selection needs to be carefully chosen with the inherent preferences and properties of the target of interest taken into consideration. As a result, we next performed a selection on TEV protease with an improved workflow. First, we used a Cys(NNK)_nCys library ($n = 9, 12, 15$; NNK library) to improve the coverage of both amino acids (20 out of 20 natural amino acids are possible using this randomization approach) and lengths. Second, inspired by previous optimizations of mRNA display,^{51,52} we replaced the first oligo-dT purification with HA tag-mediated enrichment after the *in vitro* translation step to ensure that only species with intact HA tag sequences are carried forward. We performed selections starting with $\sim 5 \times 10^{12}$ unique sequences through binding to the immobilized TEV protease. As in our initial selection, we incubated the library with TEV protease overnight in the first two rounds, then 1 h in the rest,

counterselected with empty streptavidin beads in the last five rounds, and performed a denaturing wash with 5 M guanidine in all rounds. Starting from the third round, we added an extra counter selection, an excess of a “dead” TEV protease mutant (C151A), during panning to remove any binders that prefer surface-exposed cysteine residues on the TEV protease (Figure 2A) and bias selections to the active site. In total, we conducted six rounds of selection until we observed a constant increase in cDNA recovery (Figure S5A). To evaluate the selection, we performed a comparative pulldown following the sixth round using the same modified library pool against several negative controls (e.g., empty beads or an easily precipitated membrane protein such as ZDHHC2), along with the positive selection (TEV protease). We also enriched the unmodified pool against TEV protease (Figure S5B). Positive selection resulted in 1.398% cDNA recovery, significantly more than any of the other negative controls tested, indicating the

enrichment is specific to TEV protease and dependent upon linker modification (Figure S5C).

Examination of the enriched sequences by NGS revealed convergence of an $-ExLxI/V-$ motif in the NNK randomized region, flanked by two fixed cysteine residues as designed (Figure S6). This is consistent with previously reported findings.²⁶ We also noted a newly emerging motif, $-EPLC(I/V)(W/Y)G-$, which features a consistent third cysteine residue flanking an $(I/V)(W/Y)G$ motif with the C-terminal cysteine. To eliminate nonspecific binders, we only selected the TEV protease-preferred, but not negative control-preferred, species among the top 20 hits in our NGS data set (Figure S7A,B), from which we synthesized five representative candidates according to multiple sequence alignment (Figures 2B and 3A). Included in this five-candidate panel was cTEV6-2, a derivative of the most enriched sequence among the conserved three-cysteine species. We inferred the C-terminal cyclization of cTEV6-2 from AlphaFold3 predictions with its parental sequences TEV6 (MCDNEPLCIWGC),⁵³ in which the EPLCIWGC sequence fits well into the substrate binding pocket of TEV protease, while the N-terminal cysteine did not engage with TEV protease (Figure S8A,B). Additionally, the two C-terminal cysteine residues are positioned in proximity to the active site C151 in TEV protease (Figure S8C), suggesting the cyclization on these two cysteine residues is more likely to result in covalent modification on the C151 on TEV protease.

We then evaluated the covalent binding properties and functional effects of the candidate panel on TEV protease activity. Of the five hits tested, we observed covalent labeling of TEV protease from cTEV2-2, 3, and 6-2 at 10 μ M via TEV protease gel shift assay, where the covalent engagement of macrocyclic molecules can be visualized by the change in size of TEV protease in denaturing SDS-PAGE followed by Western Blot (Figures 3B and S9). While we observed weak covalent labeling at 10 μ M, we did not measure any inhibition with the previously reported TEV13 at 10 μ M under these assay conditions. In addition, we observed TEV protease inhibition by those peptides capable of labeling TEV protease, including cTEV2-2, cTEV3, and cTEV6-2, at both 1 and 10 μ M (Figure 3C), confirming our mRNA display platform is able to generate inhibitors that covalently engage with the target of interest.

Calculated IC_{50} s following 1 h of preincubation confirmed that cTEV2-2 (6.65 μ M, 95% CI 4.281–10.39 μ M), cTEV3 (25.27 μ M, 95% CI 16.60–40.12 μ M), and cTEV6-2 (81.7 nM, 95% CI 65.6–102 nM) are more potent inhibitors than TEV13 (>50 μ M). In addition, time-resolved IC_{50} decreases for cTEV2-2, cTEV3, and cTEV6-2 from TEV protease selection are in line with the feature of covalent inhibition (Figures 4A and S10). We therefore focused our next efforts on cTEV6-2, which is the best performer in both our initial labeling screen and IC_{50} measurements.

cTEV6-2 as Potent Covalent Inhibitor Targeting the Active Site of TEV Protease. We first measured the k_{inact}/K_i of cTEV6-2 on TEV protease as $7.70 \times 10^5 \text{ M}^{-1} \text{ min}^{-1}$ (Figure S11), which is consistent with rapid inhibitory saturation of TEV protease. We then assessed the mechanism of the inhibition of cTEV6-2. A gel shift assay with TEV protease and the C151A dead mutant confirmed that cTEV6-2 exclusively labels the active site cysteine residue (Figure 4B). This observation is in line with the AlphaFold3 modeling we performed with TEV6 (MCDNEPLCIWGC) during validation,⁵³ confirming computational predictions can help in

determining the structure of cyclic peptide inhibitors. In addition, from prediction alignment, we found that the core motif of linear TEV6 resembles both the TEV protease substrate (ENLYFQS) and the linear form of TEV13 (ACFMQEPLYICG). Specifically, TEV6 overlaps with the $-QEPL-$ motif in linear TEV13, and the C-terminal of TEV6 can mimic the glutamine residue in the TEV protease substrate (Figure S8D).

To further evaluate the necessity of covalency, we synthesized and tested ncTEV6-2, in which the vinyl sulfone warhead is reduced to an ethyl sulfone (Figure 4C). Although ncTEV6-2 is a stronger inhibitor of TEV protease than iodoacetamide-alkyne (IA-alkyne), a promiscuous cysteine-targeting probe that did not inhibit TEV protease up to 50 μ M (Figure S13A), ncTEV6-2, showed significantly reduced potency than cTEV6-2 (Figure 4D), with an IC_{50} = 19.45 μ M (95% CI 14.43–26.93 μ M) upon 1 h of preincubation, indicating the covalent warhead is required for the strong inhibition of cTEV6-2. To investigate the specificity of cTEV6-2, we challenged human cathepsins S and L, two human cysteine hydrolases, with cTEV6-2 *in vitro*, which showed IC_{50} s > 50 μ M upon 1 h treatment with cTEV6-2 (Figure S12). To further evaluate the proteome-wise specificity of cTEV6-2, we incubated 1 μ M cTEV6-2 with HEK293T cell lysate with or without a 100 nM TEV protease spike-in for 1 h, followed by treatment with a dose gradient of cysteine-targeting iodoacetamide-fluorescein (IA-FITC) (Figure S13B). IA-FITC showed strong labeling in HEK293T cell lysate but no labeling on TEV protease, which aligns with our *in vitro* enzymatic assay results with IA-alkyne. We also observed complete modification of TEV protease in cell lysate upon 1 h treatment with 1 μ M cTEV6-2, with no fluorescence loss from IA-FITC labeling across the proteome (Figure S13C), suggesting while cTEV6-2 covalently binds to TEV protease with high affinity, it has minimal significant covalent off-targets in the human proteome. Overall, these data demonstrate that our optimized mRNA display workflow can generate potent and specific covalent inhibitors to TEV protease.

CONCLUSIONS

Taken together, this study showcases a strategy to apply mRNA display for selecting covalent enzyme inhibitors with high site-specificity and potency by chemical functionalization with DBA-VS, a trireactive linker with a bis-electrophilic cyclizing moiety. Our case study of TEV demonstrates that the combination of mRNA display and DBA-VS linker-mediated functionalization yields covalent macrocyclic peptide ligands that effectively target the active site of a model cysteine hydrolase. Compared with phage display,²⁶ we identified cTEV6-2, a noncanonical C-terminal-cyclizing macrocycle that is the most potent inhibitor of TEV protease currently described, without the need for secondary sequence optimization. The distinct cyclic structures of three covalent inhibitors identified in this study – cTEV2-2, cTEV3, and cTEV6-2 – also suggest the potential of mRNA display to identify structurally diverse covalent macrocyclic ligands from a single selection. Resonating with other work expanding the chemical potential of mRNA display,^{32,54} our work with TEV protease showcases the power of using the vast library sizes and diversity possible with mRNA display to identify scaffolds for potent covalent inhibition.

Our study also raises important technical considerations that warrant careful evaluation in future applications. For our TEV

protease selections, we observed an enrichment of conserved three-cysteine species (Supporting Information Figure S6), which might result in the coexistence of multiple cyclic structures, with or without covalent warhead, originating from the same sequence during the selection. We demonstrated the feasibility of identifying the effective covalent targeting structure using a computation-assisted approach. Specifically, we predicted the structure of cTEV6-2 using AlphaFold3 on the parental linear sequence TEV6 to inform and prioritize molecules for secondary screens. Additionally, the innate preferences of a target of interest for a particular macrocycle size are critical. Intriguingly, we found that both cTEV6-2 and cTEV2-2, the molecules with the strongest covalent inhibition in our screen, share a five-amino acid residue cyclic structure. Finally, the possible formation of cyclic structures without a covalent warhead (for example, a bicyclic peptide with all three-cysteine residues reacted with the same DBA-VS linker) necessitates the need of a denaturing washing step in every round of selection for covalent ligands, as was found in the previous studies.²⁹

The workflow described in this study can be further adapted for broad diversification with nucleic acid- and peptide-compatible chemistry in the mRNA display. For example, covalent warheads targeting other nucleophilic moieties in biomolecules,^{55,56} like serine or lysine,^{26,33} can be introduced to the mRNA display platform via cyclization using similar library and linker design. While not tested in the current study, our workflow in principle can also be used to directly integrate late-stage chemical modifications into mRNA display for diverse purposes.^{38,57–61} We demonstrated the success of peptide chemical modification without interference from other mRNA display components by oligo-dT- and HA tag-mediated separations. Although this required additional steps, we showed that these modifications of the mRNA display library can nonetheless be achieved within several hours. In addition, the high separation efficiency and ease of operation make these separations suitable for automation, ostensibly reducing the overall labor. Moving forward, we anticipate that the strategy outlined in this study will complement current mRNA display toolkits and help expand the scope of ligandability and ligandable targets for future chemical probe development and drug discovery.

■ ASSOCIATED CONTENT

SI Supporting Information

The Supporting Information is available free of charge at <https://pubs.acs.org/doi/10.1021/jacs.4c07851>.

Setting up an mRNA display platform for covalent macrocyclic ligand discovery; quantification of TEV protease cleavage assay assessing cyclization efficiency of DBA-VS and DCA-VS; selection with Cys(NNU)9Cys library with TEV protease; top 50 hits from TEV protease selection using Cys(NNU)9Cys library; additional data of TEV protease selection with Cys(NNK)-nCys library; top 50 hits from TEV protease selection using Cys(NNK)nCys library; analysis of TEV protease-preferred sequences from the NGS dataset; AlphaFold3-predicted binding model of linear TEV6 peptide with TEV protease; higher contrast Western Blot showing covalent engagement of macrocyclic molecules; time-course effects of cTEV2-2, cTEV3, cTEV6-2, and TEV13 on TEV protease activity; kinetic analysis of

cTEV6-2 on TEV protease; effect of cTEV6-2 on cathepsin L and S activity; competitive labeling of cTEV6-2 with iodoacetamide-fluorescein in HEK293T cell lysate; sequences of DNA oligos used in this study; amino acid sequences of proteins used in this study; methods; and spectra (PDF)

■ AUTHOR INFORMATION

Corresponding Author

Bryan C. Dickinson – Department of Chemistry, The University of Chicago, Chicago, Illinois 60637, United States; Chan Zuckerberg Biohub, Chicago, Illinois 60642, United States; orcid.org/0000-0002-9616-1911; Email: Dickinson@uchicago.edu

Authors

- Tong Lan** – Department of Chemistry, The University of Chicago, Chicago, Illinois 60637, United States; orcid.org/0000-0003-3923-5408
- Cheng Peng** – Department of Chemistry, The University of Chicago, Chicago, Illinois 60637, United States
- Xiyuan Yao** – Department of Chemistry, The University of Chicago, Chicago, Illinois 60637, United States; orcid.org/0000-0002-2331-0023
- Rachel Shu Ting Chan** – Department of Chemistry, The University of Chicago, Chicago, Illinois 60637, United States
- Tongyao Wei** – Department of Chemistry, The University of Chicago, Chicago, Illinois 60637, United States
- Anuchit Rupanya** – Department of Chemistry, The University of Chicago, Chicago, Illinois 60637, United States
- Aleksandar Radakovic** – Department of Chemistry, The University of Chicago, Chicago, Illinois 60637, United States
- Sijie Wang** – Department of Pathology, Stanford University School of Medicine, Stanford, California 94305, United States
- Shiyu Chen** – Department of Pathology, Stanford University School of Medicine, Stanford, California 94305, United States; Present Address: Biotech Drug Research Center, Shanghai Institute of Materia Medica, Chinese Academy of Sciences, Shanghai 201203, China; orcid.org/0000-0001-6578-561X
- Scott Lovell** – Department of Pathology, Stanford University School of Medicine, Stanford, California 94305, United States; Present Address: Department of Biology and Biochemistry, University of Bath, Claverton Down, Bath BA2 7AY, United Kingdom.
- Scott A. Snyder** – Department of Chemistry, The University of Chicago, Chicago, Illinois 60637, United States; orcid.org/0000-0003-3594-8769
- Matthew Bogyo** – Department of Pathology and Department of Microbiology and Immunology, Stanford University School of Medicine, Stanford, California 94305, United States; orcid.org/0000-0003-3753-4412

Complete contact information is available at: <https://pubs.acs.org/doi/10.1021/jacs.4c07851>

Notes

The authors declare no competing financial interest.

■ ACKNOWLEDGMENTS

This work was supported by the National Institute of General Medical Sciences of the National Institutes of Health NIH

(R35 GM119840 to B.C.D.). We thank S. Ahmadiantehrani for editing assistance and Y. Cao and R. Sinnott for technical assistance. We thank the University of Chicago Comprehensive Cancer Center DNA Sequencing and Genotyping Facility for sequencing services.

REFERENCES

- (1) Boike, L.; Henning, N. J.; Nomura, D. K. Advances in covalent drug discovery. *Nat. Rev. Drug Discov* **2022**, *21* (12), 881–898.
- (2) Singh, J.; Petter, R. C.; Baillie, T. A.; Whitty, A. The resurgence of covalent drugs. *Nat. Rev. Drug Discov* **2011**, *10* (4), 307–317.
- (3) Knight, Z. A.; Lin, H.; Shokat, K. M. Targeting the cancer kinome through polypharmacology. *Nat. Rev. Cancer* **2010**, *10* (2), 130–137.
- (4) Weerapana, E.; Wang, C.; Simon, G. M.; Richter, F.; Khare, S.; Dillon, M. B.; Bachovchin, D. A.; Mowen, K.; Baker, D.; Cravatt, B. F. Quantitative reactivity profiling predicts functional cysteines in proteomes. *Nature* **2010**, *468* (7325), 790–795.
- (5) Backus, K. M.; Correia, B. E.; Lum, K. M.; Forli, S.; Horning, B. D.; Gonzalez-Paez, G. E.; Chatterjee, S.; Lanning, B. R.; Teijaro, J. R.; Olson, A. J.; Wolan, D. W.; Cravatt, B. F. Proteome-wide covalent ligand discovery in native biological systems. *Nature* **2016**, *534* (7608), 570–574.
- (6) Vinogradova, E. V.; Zhang, X.; Remillard, D.; Lazar, D. C.; Suci, R. M.; Wang, Y.; Bianco, G.; Yamashita, Y.; Crowley, V. M.; Schafroth, M. A.; Yokoyama, M.; Konrad, D. B.; Lum, K. M.; Simon, G. M.; Kemper, E. K.; Lazear, M. R.; Yin, S.; Blewett, M. M.; Dix, M. M.; Nguyen, N.; Shokhirev, M. N.; Chin, E. N.; Lairson, L. L.; Melillo, B.; Schreiber, S. L.; Forli, S.; Teijaro, J. R.; Cravatt, B. F. An Activity-Guided Map of Electrophile-Cysteine Interactions in Primary Human T Cells. *Cell* **2020**, *182* (4), 1009–1026. e29
- (7) Kemper, E. K.; Zhang, Y.; Dix, M. M.; Cravatt, B. F. Global profiling of phosphorylation-dependent changes in cysteine reactivity. *Nat. Methods* **2022**, *19* (3), 341–352.
- (8) Takahashi, M.; Chong, H. B.; Zhang, S.; Yang, T. Y.; Lazarov, M. J.; Harry, S.; Maynard, M.; Hilbert, B.; White, R. D.; Murrey, H. E.; Tsou, C. C.; Vordermark, K.; Assaad, J.; Gohar, M.; Durr, B. R.; Richter, M.; Patel, H.; Kryukov, G.; Brooijmans, N.; Alghali, A. S. O.; Rubio, K.; Villanueva, A.; Zhang, J.; Ge, M.; Makram, F.; Griesshaber, H.; Harrison, D.; Koglin, A. S.; Ojeda, S.; Karakyriakou, B.; Healy, A.; Popoola, G.; Rachmin, I.; Khandelwal, N.; Neil, J. R.; Tien, P. C.; Chen, N.; Hosp, T.; van den Ouweland, S.; Hara, T.; Bussema, L.; Dong, R.; Shi, L.; Rasmussen, M. Q.; Domingues, A. C.; Lawless, A.; Fang, J.; Yoda, S.; Nguyen, L. P.; Reeves, S. M.; Wakefield, F. N.; Acker, A.; Clark, S. E.; Dubash, T.; Kastanos, J.; Oh, E.; Fisher, D. E.; Maheswaran, S.; Haber, D. A.; Boland, G. M.; Sade-Feldman, M.; Jenkins, R. W.; Hata, A. N.; Bardeesy, N. M.; Suva, M. L.; Martin, B. R.; Liau, B. B.; Ott, C. J.; Rivera, M. N.; Lawrence, M. S.; Bar-Peled, L. DrugMap: A quantitative pan-cancer analysis of cysteine ligandability. *Cell* **2024**, *187* (10), 2536–2556.e30.
- (9) Li, H.; Ma, T.; Remsberg, J. R.; Won, S. J.; DeMeester, K. E.; Njomen, E.; Ogasawara, D.; Zhao, K. T.; Huang, T. P.; Lu, B.; Simon, G. M.; Melillo, B.; Schreiber, S. L.; Lykke-Andersen, J.; Liu, D. R.; Cravatt, B. F. Assigning functionality to cysteines by base editing of cancer dependency genes. *Nat. Chem. Biol.* **2023**, *19* (11), 1320–1330.
- (10) Tao, Y.; Felber, J. G.; Zou, Z.; Njomen, E.; Remsberg, J. R.; Ogasawara, D.; Ye, C.; Melillo, B.; Schreiber, S. L.; He, C.; Remillard, D.; Cravatt, B. F. Chemical Proteomic Discovery of Isotype-Selective Covalent Inhibitors of the RNA Methyltransferase NSUN2. *Angew. Chem., Int. Ed. Engl.* **2023**, *62* (51), No. e202311924.
- (11) Lazear, M. R.; Remsberg, J. R.; Jaeger, M. R.; Rothamel, K.; Her, H. L.; DeMeester, K. E.; Njomen, E.; Hogg, S. J.; Rahman, J.; Whitby, L. R.; Won, S. J.; Schafroth, M. A.; Ogasawara, D.; Yokoyama, M.; Lindsey, G. L.; Li, H.; Germain, J.; Barbas, S.; Vaughan, J.; Hanigan, T. W.; Vartabedian, V. F.; Reinhardt, C. J.; Dix, M. M.; Koo, S. J.; Heo, I.; Teijaro, J. R.; Simon, G. M.; Ghosh, B.; Abdel-Wahab, O.; Ahn, K.; Saghatelian, A.; Melillo, B.; Schreiber, S. L.; Yeo, G. W.; Cravatt, B. F. Proteomic discovery of chemical probes that perturb protein complexes in human cells. *Mol. Cell* **2023**, *83* (10), 1725–1742. e12
- (12) Vinogradov, A. A.; Yin, Y.; Suga, H. Macrocyclic Peptides as Drug Candidates: Recent Progress and Remaining Challenges. *J. Am. Chem. Soc.* **2019**, *141* (10), 4167–4181.
- (13) Zorzi, A.; Deyle, K.; Heinis, C. Cyclic peptide therapeutics: past, present and future. *Curr. Opin. Chem. Biol.* **2017**, *38*, 24–29.
- (14) Josephson, K.; Ricardo, A.; Szostak, J. W. mRNA display: from basic principles to macrocycle drug discovery. *Drug Discov Today* **2014**, *19* (4), 388–99.
- (15) Ji, X.; Nielsen, A. L.; Heinis, C. Cyclic Peptides for Drug Development. *Angew. Chem., Int. Ed. Engl.* **2024**, *63* (3), No. e202308251.
- (16) Goto, Y.; Suga, H. The RaPID Platform for the Discovery of Pseudo-Natural Macrocyclic Peptides. *Acc. Chem. Res.* **2021**, *54* (18), 3604–3617.
- (17) Zhang, G.; Brown, J. S.; Quartararo, A. J.; Li, C.; Tan, X.; Hanna, S.; Antilla, S.; Cowfer, A. E.; Loas, A.; Pentelute, B. L. Rapid de novo discovery of peptidomimetic affinity reagents for human angiotensin converting enzyme 2. *Commun. Chem.* **2022**, *5* (1), 8.
- (18) Chen, F. J.; Pinnette, N.; Gao, J. Strategies for the Construction of Multicyclic Phage Display Libraries. *ChemBioChem* **2024**, *25* (9), No. e202400072.
- (19) Derda, R.; Ng, S. Genetically encoded fragment-based discovery. *Curr. Opin. Chem. Biol.* **2019**, *50*, 128–137.
- (20) Dong, H.; Li, J.; Liu, H.; Lu, S.; Wu, J.; Zhang, Y.; Yin, Y.; Zhao, Y.; Wu, C. Design and Ribosomal Incorporation of Non-canonical Disulfide-Directing Motifs for the Development of Multicyclic Peptide Libraries. *J. Am. Chem. Soc.* **2022**, *144* (11), 5116–5125.
- (21) Iqbal, E. S.; Hartman, M. C. T. Shaping molecular diversity. *Nat. Chem.* **2018**, *10* (7), 692–694.
- (22) Sohrabi, C.; Foster, A.; Tavassoli, A. Methods for generating and screening libraries of genetically encoded cyclic peptides in drug discovery. *Nat. Rev. Chem.* **2020**, *4* (2), 90–101.
- (23) Kamalinia, G.; Grindel, B. J.; Takahashi, T. T.; Millward, S. W.; Roberts, R. W. Directing evolution of novel ligands by mRNA display. *Chem. Soc. Rev.* **2021**, *50* (16), 9055–9103.
- (24) Iskandar, S. E.; Bowers, A. A. mRNA Display Reaches for the Clinic with New PCSK9 Inhibitor. *ACS Med. Chem. Lett.* **2022**, *13* (9), 1379–1383.
- (25) Howard, J. F., Jr.; Vissing, J.; Gilhus, N. E.; Leite, M. I.; Utsugisawa, K.; Duda, P. W.; Farzaneh-Far, R.; Murai, H.; Wiendl, H. Zilucoplan: An Investigational Complement C5 Inhibitor for the Treatment of Acetylcholine Receptor Autoantibody-Positive Generalized Myasthenia Gravis. *Expert Opin Investig Drugs* **2021**, *30* (5), 483–493.
- (26) Chen, S.; Lovell, S.; Lee, S.; Fellner, M.; Mace, P. D.; Bogyo, M. Identification of highly selective covalent inhibitors by phage display. *Nat. Biotechnol.* **2021**, *39* (4), 490–498.
- (27) Ekanayake, A. I.; Sobze, L.; Kelich, P.; Youk, J.; Bennett, N. J.; Mukherjee, R.; Bhardwaj, A.; Wuest, F.; Vukovic, L.; Derda, R. Genetically Encoded Fragment-Based Discovery from Phage-Displayed Macrocyclic Libraries with Genetically Encoded Unnatural Pharmacophores. *J. Am. Chem. Soc.* **2021**, *143* (14), 5497–5507.
- (28) Tabuchi, Y.; Watanabe, T.; Katsuki, R.; Ito, Y.; Taki, M. Direct screening of a target-specific covalent binder: stringent regulation of warhead reactivity in a matchmaking environment. *Chem. Commun. (Camb)* **2021**, *57* (44), 5378–5381.
- (29) Iskandar, S. E.; Chiou, L. F.; Leisner, T. M.; Shell, D. J.; Norris-Drouin, J. L.; Vaziri, C.; Pearce, K. H.; Bowers, A. A. Identification of Covalent Cyclic Peptide Inhibitors in mRNA Display. *J. Am. Chem. Soc.* **2023**, *145* (28), 15065–15070.
- (30) Norman, A.; Franck, C.; Christie, M.; Hawkins, P. M. E.; Patel, K.; Ashhurst, A. S.; Aggarwal, A.; Low, J. K. K.; Siddiquee, R.; Ashley, C. L.; Steain, M.; Triccas, J. A.; Turville, S.; Mackay, J. P.; Passioura, T.; Payne, R. J. Discovery of Cyclic Peptide Ligands to the SARS-

- CoV-2 Spike Protein Using mRNA Display. *ACS Cent Sci.* **2021**, *7* (6), 1001–1008.
- (31) Wu, Y.; Bertran, M. T.; Joshi, D.; Maslen, S. L.; Hurd, C.; Walport, L. J. Identification of photocrosslinking peptide ligands by mRNA display. *Commun. Chem.* **2023**, *6* (1), 103.
- (32) Peacock, H.; Suga, H. Discovery of De Novo Macrocyclic Peptides by Messenger RNA Display. *Trends Pharmacol. Sci.* **2021**, *42* (5), 385–397.
- (33) Zheng, M.; Chen, F. J.; Li, K.; Reja, R. M.; Haeffner, F.; Gao, J. Lysine-Targeted Reversible Covalent Ligand Discovery for Proteins via Phage Display. *J. Am. Chem. Soc.* **2022**, *144* (34), 15885–15893.
- (34) Hampton, J. T.; Liu, W. R. Diversification of Phage-Displayed Peptide Libraries with Noncanonical Amino Acid Mutagenesis and Chemical Modification. *Chem. Rev.* **2024**, *124* (9), 6051–6077.
- (35) Diderich, P.; Bertoldo, D.; Dessen, P.; Khan, M. M.; Pizzitola, I.; Held, W.; Huelsken, J.; Heinis, C. Phage Selection of Chemically Stabilized alpha-Helical Peptide Ligands. *ACS Chem. Biol.* **2016**, *11* (5), 1422–7.
- (36) Jafari, M. R.; Lakusta, J.; Lundgren, R. J.; Derda, R. Allene Functionalized Azobenzene Linker Enables Rapid and Light-Responsive Peptide Macrocyclization. *Bioconjug Chem.* **2016**, *27* (3), 509–14.
- (37) Kalhor-Monfared, S.; Jafari, M. R.; Patterson, J. T.; Kitov, P. I.; Dwyer, J. J.; Nuss, J. M.; Derda, R. Rapid biocompatible macrocyclization of peptides with decafluoro-diphenylsulfone. *Chem. Sci.* **2016**, *7* (6), 3785–3790.
- (38) Schlippe, Y. V.; Hartman, M. C.; Josephson, K.; Szostak, J. W. In vitro selection of highly modified cyclic peptides that act as tight binding inhibitors. *J. Am. Chem. Soc.* **2012**, *134* (25), 10469–77.
- (39) Hacker, D. E.; Hoinka, J.; Iqbal, E. S.; Przytycka, T. M.; Hartman, M. C. Highly Constrained Bicyclic Scaffolds for the Discovery of Protease-Stable Peptides via mRNA Display. *ACS Chem. Biol.* **2017**, *12* (3), 795–804.
- (40) Abrigo, N. A.; Dods, K. K.; Makovsky, C. A.; Lohan, S.; Mitra, K.; Newcomb, K. M.; Le, A.; Hartman, M. C. T. Development of a Cyclic, Cell Penetrating Peptide Compatible with In Vitro Selection Strategies. *ACS Chem. Biol.* **2023**, *18* (4), 746–755.
- (41) Villequey, C.; Zurmühl, S. S.; Cramer, C. N.; Bhusan, B.; Andersen, B.; Ren, Q.; Liu, H.; Qu, X.; Yang, Y.; Pan, J.; Chen, Q.; Münzel, M. An efficient mRNA display protocol yields potent bicyclic peptide inhibitors for FGFR3c: outperforming linear and monocyclic formats in affinity and stability. *Chemical Science* **2024**, *15* (16), 6122–6129.
- (42) Alleyne, C.; Amin, R. P.; Bhatt, B.; Bianchi, E.; Blain, J. C.; Boyer, N.; Branca, D.; Embrey, M. W.; Ha, S. N.; Jette, K.; Johns, D. G.; Kerekes, A. D.; Koeplinger, K. A.; LaPlaca, D.; Li, N.; Murphy, B.; Orth, P.; Ricardo, A.; Salowe, S.; Seyb, K.; Shahripour, A.; Stringer, J. R.; Sun, Y.; Tracy, R.; Wu, C.; Xiong, Y.; Youm, H.; Zokian, H. J.; Tucker, T. J. Series of Novel and Highly Potent Cyclic Peptide PCSK9 Inhibitors Derived from an mRNA Display Screen and Optimized via Structure-Based Design. *J. Med. Chem.* **2020**, *63* (22), 13796–13824.
- (43) Newton, M. S.; Cabezas-Perusse, Y.; Tong, C. L.; Seelig, B. In Vitro Selection of Peptides and Proteins—Advantages of mRNA Display. *ACS Synth. Biol.* **2020**, *9* (2), 181–190.
- (44) Seelig, B. mRNA display for the selection and evolution of enzymes from in vitro-translated protein libraries. *Nat. Protoc.* **2011**, *6* (4), 540–52.
- (45) Grindel, B. J.; Engel, B. J.; Ong, J. N.; Srinivasamani, A.; Liang, X.; Zacharias, N. M.; Bast, R. C., Jr; Curran, M. A.; Takahashi, T. T.; Roberts, R. W.; Millward, S. W. Directed Evolution of PD-L1-Targeted Affibodies by mRNA Display. *ACS Chem. Biol.* **2022**, *17* (6), 1543–1555.
- (46) Reyes, S. G.; Kuruma, Y.; Fujimi, M.; Yamazaki, M.; Eto, S.; Nishikawa, S.; Tamaki, S.; Kobayashi, A.; Mizuuchi, R.; Rothschild, L.; Ditzler, M.; Fujishima, K. PURE mRNA display and cDNA display provide rapid detection of core epitope motif via high-throughput sequencing. *Biotechnol. Bioeng.* **2021**, *118* (4), 1736–1749.
- (47) Roberts, R. W.; Szostak, J. W. RNA-peptide fusions for the in vitro selection of peptides and proteins. *Proc. Natl. Acad. Sci. U. S. A.* **1997**, *94* (23), 12297–302.
- (48) Liu, R.; Barrick, J. E.; Szostak, J. W.; Roberts, R. W. Optimized synthesis of RNA-protein fusions for in vitro protein selection. *Methods Enzymol.* **2000**, *318*, 268–93.
- (49) Lewis, Y. E.; Abeywardana, T.; Lin, Y. H.; Galesic, A.; Pratt, M. R. Synthesis of a Bis-thio-acetone (BTA) Analogue of the Lysine Isopeptide Bond and its Application to Investigate the Effects of Ubiquitination and SUMOylation on alpha-Synuclein Aggregation and Toxicity. *ACS Chem. Biol.* **2016**, *11* (4), 931–42.
- (50) Yamagishi, Y.; Shoji, I.; Miyagawa, S.; Kawakami, T.; Katoh, T.; Goto, Y.; Suga, H. Natural product-like macrocyclic N-methyl-peptide inhibitors against a ubiquitin ligase uncovered from a ribosome-expressed de novo library. *Chem. Biol.* **2011**, *18* (12), 1562–70.
- (51) Fleming, S. R.; Himes, P. M.; Ghodge, S. V.; Goto, Y.; Suga, H.; Bowers, A. A. Exploring the Post-translational Enzymology of PaaA by mRNA Display. *J. Am. Chem. Soc.* **2020**, *142* (11), 5024–5028.
- (52) Bowler, M. M.; Glavatskikh, M.; Pecot, C. V.; Kireev, D.; Bowers, A. A. Enzymatic Macrolactamization of mRNA Display Libraries for Inhibitor Selection. *ACS Chem. Biol.* **2023**, *18* (1), 166–175.
- (53) Abramson, J.; Adler, J.; Dunger, J.; Evans, R.; Green, T.; Pritzel, A.; Ronneberger, O.; Willmore, L.; Ballard, A. J.; Bambrick, J.; Bodenstein, S. W.; Evans, D. A.; Hung, C.-C.; O’Neill, M.; Reiman, D.; Tunyasuvunakool, K.; Wu, Z.; Žemgulytė, A.; Arvaniti, E.; Beattie, C.; Bertolli, O.; Bridgland, A.; Cherepanov, A.; Congreve, M.; Cowen-Rivers, A. I.; Cowie, A.; Figurnov, M.; Fuchs, F. B.; Gladman, H.; Jain, R.; Khan, Y. A.; Low, C. M. R.; Perlin, K.; Potapenko, A.; Savy, P.; Singh, S.; Stecula, A.; Thillaisundaram, A.; Tong, C.; Yakneen, S.; Zhong, E. D.; Zielinski, M.; Židek, A.; Bapst, V.; Kohli, P.; Jaderberg, M.; Hassabis, D.; Jumper, J. M. Accurate structure prediction of biomolecular interactions with AlphaFold 3. *Nature* **2024**, *630*, 493–500.
- (54) Huang, Y.; Wiedmann, M. M.; Suga, H. RNA Display Methods for the Discovery of Bioactive Macrocycles. *Chem. Rev.* **2019**, *119* (17), 10360–10391.
- (55) McCarthy, K. A.; Kelly, M. A.; Li, K.; Cambray, S.; Hosseini, A. S.; van Opijnen, T.; Gao, J. Phage Display of Dynamic Covalent Binding Motifs Enables Facile Development of Targeted Antibiotics. *J. Am. Chem. Soc.* **2018**, *140* (19), 6137–6145.
- (56) Wang, N.; Yang, B.; Fu, C.; Zhu, H.; Zheng, F.; Kobayashi, T.; Liu, J.; Li, S.; Ma, C.; Wang, P. G.; Wang, Q.; Wang, L. Genetically Encoding Fluorosulfate-L-tyrosine To React with Lysine, Histidine, and Tyrosine via SuFEx in Proteins in Vivo. *J. Am. Chem. Soc.* **2018**, *140* (15), 4995–4999.
- (57) Bhattarai, U.; Hsieh, W. C.; Yan, H.; Guo, Z. F.; Shaikh, A. Y.; Soltani, A.; Song, Y.; Ly, D. H.; Liang, F. S. Bifunctional small molecule-oligonucleotide hybrid as microRNA inhibitor. *Bioorg. Med. Chem.* **2020**, *28* (7), No. 115394.
- (58) Cui, X. Y.; Li, Z.; Kong, Z.; Liu, Y.; Meng, H.; Wen, Z.; Wang, C.; Chen, J.; Xu, M.; Li, Y.; Gao, J.; Zhu, W.; Hao, Z.; Huo, L.; Liu, S.; Yang, Z.; Liu, Z. Covalent targeted radioligands potentiate radionucleclide therapy. *Nature* **2024**, *630*, 206–213.
- (59) Lin, C. L.; Sojitra, M.; Carpenter, E. J.; Hayhoe, E. S.; Sarkar, S.; Volker, E. A.; Wang, C.; Bui, D. T.; Yang, L.; Klassen, J. S.; Wu, P.; Macauley, M. S.; Lowary, T. L.; Derda, R. Chemoenzymatic synthesis of genetically-encoded multivalent liquid N-glycan arrays. *Nat. Commun.* **2023**, *14* (1), 5237.
- (60) Liu, C.; Liu, X.; Zhou, M.; Xia, C.; Lyu, Y.; Peng, Q.; Soni, C.; Zhou, Z.; Su, Q.; Wu, Y.; Weerapana, E.; Gao, J.; Chatterjee, A.; Lin, C.; Niu, J. Fluorosulfate as a Latent Sulfate in Peptides and Proteins. *J. Am. Chem. Soc.* **2023**, *145* (37), 20189–20195.
- (61) Wu, L.; Zhou, Z.; Sathe, D.; Zhou, J.; Dym, S.; Zhao, Z.; Wang, J.; Niu, J. Precision native polysaccharides from living polymerization of anhydrosugars. *Nat. Chem.* **2023**, *15* (9), 1276–1284.